NASA Contractor Report 172595

NASA-CR-172595
19850020201

Solar Radiance Models for Determination of ERBE Scanner Filter Factor

R. F. Arduini

Information & Control Systems, Incorporated
Hampton, VA 23666

Contract NAS1-17425
Interim Report

May 1985

National Aeronautics and Space Administration

Langley Research Center
Hampton, Virginia 23665

ABSTRACT

The purpose of this effort has been to provide shortwave spectral radiance models for use in the spectral correction algorithms for the ERBE Scanner Instrument. The required data base was delivered to the ERBE Data Reduction Group in October, 1984. It consisted of two sets of data files: (1) the spectral bidirectional angular models and (2) the spectral flux models. The bidirectional models embody the angular characteristics of reflection by the Earth-atmosphere system and were derived from detailed radiance calculations using a finite difference model of the radiative transfer process. The spectral flux models were created through the use of a delta-Eddington model to economically simulate the effects of atmospheric variability. By combining these data sets, a wide range of radiances may be approximated for a number of scene types.

TABLE OF CONTENTS

LIST OF TABLES

LIST OF FIGURES

I. INTRODUCTION

The algorithm being used to compute the spectral correction coefficients for the Earth Radiation Budget Experiment (ERBE) Scanner instruments requires a priori models of the spectral radiance at the top of the atmosphere (TOA) being sampled by the instruments. The purpose of this work therefore has been to provide those shortwave models (0.25 - 5.0 μm) through the use of well-established radiative transfer techniques combined with the most realistic input data available. The approach decided upon has been to use a detailed finite difference code to compute the TOA radiances to determine spectral angular bidirectional models for each of the surface and sun angle combinations with "mean" atmospheric conditions. At this point an approximate (delta-Eddington) code could be used to compute the upwelling spectral flux at the top of the atmosphere for the same surface - sun angle combinations but for a wide range of atmospheric conditions. Then by combining the fluxes with the appropriate angular directional models the complete spectral radiance models for all the desired atmosphere-surface-sun angle combinations may be approximated. This approach minimizes the use of the finite difference code which is very expensive in terms of computer costs. The final products therefore consist of a set of data files of spectral bidirectional models for each surface-sun angle combination and a set of files containing the spectral flux models. Together these files form a data base which may be used to provide the necessary radiances for the shortwave spectral correction algorithms.

This report briefly summarizes the work which resulted in the above products. It begins with a discussion of the development of a case list which was based on the availability of data (both surface reflectance and atmospheric data) and on a desire to minimize the number of full radiance calculations

required due to the expense involved in running the finite difference code. This is followed by a brief description of the finite difference program, FD, with an emphasis on the implementation of the spectral, bidirectional reflectance data. Next is a discussion of the use of delta-Eddington code to compute the upwelling flux at TOA. The report ends with a description and examples of the data products which have been delivered for use in the scanner spectral correction algorithms.

A follow on effort is planned in which all of the details of the computations involved here will be presented and documented in a volume of the ERBE Science Reference Manual.

II. DETERMINATION OF SURFACE-ATMOSPHERE CASE STUDIES

Regardless of the efficiency of the method used, any comprehensive computation of the radiance distribution at the top of the Earth's atmosphere is a costly endeavor in terms of computer time and resources. The processes involved in describing the transfer of solar radiation through a variable atmosphere, the reflection by a wide variety of surfaces and the dependencies of these processes upon wavelength and illumination-viewing geometry make such a computation difficult at best.

The requirement here is that just such a computation be made in order to provide a global data base of radiances for use in deriving the ERBE Scanner spectral correction coefficients. This data base needs to include examples of as many of the most common scene types visible from space as is practical. In addition, atmospheric variations can have important effects on the radiance distribution and so it is desirable to include as many typical atmospheres as possible in the data base. Add to this the variation with solar zenith angle and it becomes evident that the number of cases can grow very quickly. With the large number of cases and the expense involved in making the radiance calculations it becomes important to judiciously select the cases to be run.

A. Initial Approach:

This rationale provided the motivation for the initial study in this work, namely to develop a comprehensive set of case studies (i. e., scene type - atmosphere combinations) and still keep the number of full radiance calculations to a minimum. The initial approach was to examine the spectra of the upwelling flux cases which were similar to the required data sets and to establish some measure of the similarity between differing scenes. For example, if it could be shown that a forest surface and a grass surface produced similar upwelling

flux spectra under a range of atmospheric conditions, then, perhaps, the two scene types could be combined into one. If further similarities could be established in their angular responses, then an argument could be made to combine the two scene types into one for the radiance computations.

An earlier study had produced upwelling flux spectra over the required spectral range, 0.25 - 5 μm for a number of surface atmosphere cases which were similar to those required in this study. The surfaces considered included ocean, forest, grass, dark soil, light soil and snow. Spectral albedo data for these surfaces was obtained from a report by Tarnopolskiy (Ref. 1). The atmospheric data came from MSL report #10 (Ref. 2) and include measurements of the vertical profiles of pressure, temperature, water vapor ans ozone over 106 meteorological stations throughout the world. The radiative transfer calculations were performed using a delta-Eddington approximation which was based upon the work of Shettle and Weinman (Ref. 3). Examples of these spectra are shown in Figure 1.

The criterion used for comparing these spectra was a "similarity factor" defined as follows:

$$S_{i,j} = \frac{\int_0^{5\mu m} M_i(\lambda)\, M_j(\lambda)\, d\lambda}{\left[\int_0^{5\mu m} M_i^2(\lambda)\, d\lambda \int_0^{5\mu m} M_j^2(\lambda)\, d\lambda \right]^{1/2}} \qquad (1)$$

where $M_i(\lambda)$ is the spectral flux in W/m^2 for the case designated by subscript i and λ is the wavelength. This quantity has a maximum value of 1.0 when $M_i(\lambda) = M_j(\lambda)$. Combinations of cases (i, j) which are similar therefore will have $S_{i,j} \approx 1.0$.

This calculation was performed for a large number of the cases described above and results showed a high degree of similarity only for cases which had the same surface but with only slightly different atmospheric conditions. The decision was then made to use a different approach for minimizing the number of full radiance runs.

B. Spectral Bidirectional Angular-Spectral Flux Approach:

The method decided upon by which to form the required radiance models is based in the relationship between the radiance L and the flux (or radiant exitance) M through a bidirectional angular function R. This relationship may be defined as follows:

$$R_\lambda (\theta_0, \theta, \phi) = \pi L_\lambda (\theta_0, \theta, \phi) / M_\lambda(\theta_0) \qquad (2)$$

where $L_\lambda (\theta_0, \theta, \phi)$ is the spectral radiance in the viewing direction defined by zenith and azimuth angles θ and ϕ, respectively, resulting from illumination by the sun at solar zenith angle θ_0. Since the spectral flux $M_\lambda(\theta_0)$ is given by

$$M_\lambda(\theta_0) = \int_0^{2\pi} \int_0^{\pi/2} L_\lambda(\theta_0, \theta, \phi) \cos\theta \sin\theta \, d\theta \, d\phi \, , \qquad (3)$$

a normalization condition may be written

$$\pi^{-1} \int_0^{2\pi} \int_0^{\pi/2} R_\lambda(\theta_0, \theta, \phi) \cos\theta \sin\theta \, d\theta \, d\phi = 1. \qquad (4)$$

Using the definitions given above, spectral bidirectional angular models may be derived from radiance simulations for the wide range of required scene types, but for a limited set of mean atmospheric conditions. Since the spectral flux is relatively inexpensive to compute (using a delta-Eddington model) a set

of spectral flux models could be developed which would embody a great number of atmospheric variations. Then by combining the bidirectional angular models with the spectral flux models the required radiances could be approximated. This approach limits the full radiance caculations to those for only mean atmospheric conditions and allows for the bulk of the atmospheric variations to be simulated by using the relatively inexpensive flux calculations. This was the approach adopted.

C. Surface Reflectance Data:

The reflection properties of typical Earth surfaces are very complicated since they depend upon so many variables: wavelength, illumination - viewing geometry, time, etc. For this reason and because of the variety of surfaces and the problems involved with measuring these properties, sources of spectral, bidirectional reflection data are very sparse. One source of data was found to be very useful for the purposes required here, namely that of Kriebel (Ref. 4). Kriebel presents tables of spectral, bidirectional reflectance factors for four vegetated surfaces: savannah, bog, coniferous forest and pasture land, at seven narrow spectral regions (0.43, 0.52, 0.61, 0.87, 1.24, 1.66 and 2.20 μm). The tables are presented for cones of reflection formed by dividing the hemisphere into 30° azimuth angle increments and 10° zenith angle increments.

A second source of bidirectional reflectance data was a report by Davis and Cox (Ref. 5). In this report they present the results of an experiment in which measurements of the reflected radiance field over various atmospheric scene types were made using a multi-detector "bug-eye instrument" mounted on an aircraft platform and flown at an altitude of 10-12 km. The instrument had a broad-band spectral response ranging from 0.3 to 1.1 μm. The bidirectional angular models which they derived from their results were presented as

coefficients of a modified spherical harmonics expansion of the measured patterns. The data they presented for the desert sands of the Saudi Arabian Empty Quarters were used in this study.

The above sources of data are limited in their spectral resolution. Therefore, in order to obtain reasonable representations of the wavelength variations of the surfaces of interest, it was decided to use some other sources of spectral albedo data in conjunction with the bidirectional angular data described above. Tarnopolskiy (Ref. 1) provides spectral albedo curves for some of the same surfaces for which the bidirectional data is available, namely, desert sands, coniferous forest and grass or pasture land. Spectral albedo data for snow and ice was obtained from a paper by Wiscombe & Warren (Ref. 6). By renormalizing the spectral albedo data to the broad-band hemispherical albedo value computed from the bidirectional data, it was possible to approximate a spectral, bidirectional reflection model for several land surfaces: desert, forest and grass. Detailed spectral reflection data for the savannah surface was not available and so the coarse spectral resolution provided by Kriebel was used. In like manner, detailed angular reflection data for ice or snow surfaces was not available and so a Lambertian assumption was made for these cases.

The ocean surface is somewhat different from typical land surfaces due to its pronounced specular reflection peak. This reflection of the directly incident beam may be described by a Fresnel law which is given in Siegel and Howell (Ref. 7). The diffuse reflection is assumed to be Lambertian and have a spectral variation as given by Morel (Ref. 8) for "blue (desert) water".

Table 1 enumerates the surfaces decided upon for simulation in this study and lists the sources of the data used.

D. Atmospheric Data:

As stated earlier, the full radiance calculations were to be done for "mean" atmospheric conditions, with simulations of the effects of detailed atmospheric variations being reserved for spectral flux calculations. The data for use in the radiance calculations comes from a report by McClatchey et al. (Ref. 9) and are for climatological conditions as follows: 1962 standard, tropical, midlatitude summer, midlatitude winter, subarctic (designated as "polar" for this work) summer and subarctic winter. The data consists of vertical distributions of the pressure, temperature, density, water vapor and ozone concentrations.

The aerosol models used employ log-normal size distributions with parameters and compositions appropriate to continental and maritime aerosols as specified in Deepak and Gerber (Ref. 10). The vertical distribution of aerosols came from McClatchey et al. (Ref. 9) and is scaled to correspond to ground level visibilities of 5 km and 23 km.

The data used to simulate atmospheric variability in the spectral flux models was developed from a data set which was obtained from the Tiros Operational Vertical Sounder (TOVS) (Ref. 11). Data files were assembled by S. Gupta which provided monthly averages of the surface temperature, pressure, ozone burden, water vapor burden, cloud top height and vertical distribution of temperature for a 12 month period (July 1981 through June 1982) over 11 different sites. It seems reasonable to assume that these sites would have surface reflectance properties which could be approximated by the reflectance data described earlier. Table 2 enumerates these TOVS sites and the assumed scene type used to describe its reflectance properties in this work.

The obscuration of the Earth's surface by clouds provides another case of interest in providing a global data base of radiances. In the FD model clouds

are treated as a homogeneous aerosol layer with size distribution parameters as given in Stephens (Ref. 12). It was decided to simulate low, middle and high altitude clouds with optical depths of approximately 6, 12 and 20 respectively so that a range of effects could be examined. Clouds with tops below 2.5 km are considered low; between 2.5 and 5.0 km, middle; and above 5.0 km, high. Stephen's altostratus cloud droplet distribution parameters were used for the high and middle clouds and the stratocumulus II parameters used for the low clouds. The radiance field for these clouds over ocean and land (grass) surfaces were calculated as part of the data base.

E. Case List:

The resulting list of cases to be simulated using the FD radiance model are enumerated in Table 3. Four solar zenith angles were selected from the FD model's angular grid for all but the polar winter scenes where the sun remains close to the horizon. Only the two largest solar zenith angles were used for these cases. The total number of radiance cases is 102.

Table 4 lists the cases decided upon for spectral flux calculations. Both clear and cloudy cases were simulated except for the desert and ice/snow scenes. The cloud height for cloudy simulations was assigned according to the TOVS data. The solar zenith angles employed here were selected to match requirements of the spectral correction software. Considering each solar zenith angle - monthly - average atmosphere - scene type combination as a unique case, the total number of spectral flux cases comes to 1080.

III. RADIATIVE TRANSFER MODELS

As discussed above, the approach decided upon requires that full radiance calculations be done for a range of scene types and for mean, climatological atmospheric conditions so that spectral bidirectional models can be developed. These models, when combined with spectral flux models for the same scene types but for detailed atmospheric variations, could then be used to reconstruct a wide range of surface-atmosphere radiances.

A. The Finite Difference Model:

The radiative tranfer model used to compute the radiance field at the top of the atmosphere employs a finite difference technique to solve the radiative transfer equation for the Earth-atmosphere system. The model was developed by Barkstrom (Ref. 13) for solving the radiative transfer problem for a plane - parallel atmosphere with detailed vertical profiles of the physical and optical properties of the important atmospheric gases and aerosols. The model was enhanced by Suttles (Ref. 14) to include azimuthal variations, spectral varations for the entire solar wavelength rnage and specular in addition to diffuse reflection at the surface. The model has been shown to yield results which are in good agreement with satelitte radiance observations (Ref. 14).

The spectral range for which the program is set-up extends from 0.25 to 5.0 μm. This wavelength region is broken up into 73 individual wavelength grid points at which the monochromatic radiative transfer equation is solved. This spectral region contains several strongly absorbing water vapor bands and to account for the absorption in these bands an exponential sum fit is used as described in Stephens (Ref. 12). This fit requires the solution to be repeated a number of times for each of the absorbing wavelengths which brings the total number of wavelengths in the spectral grid to 96.

The angular grid consists of 15 zenith angles and 11 azimuthal angles. The azimuthal angles are measured relative to the principal plane (containing the ray from the sun to the target area) with $\phi = 0°$ corresponding to forward scatter and $\phi = 180°$ to backscatter. The zenith angle grid is chosen in such a manner as to minimize the error which results from the angular quadrature used in the solution. Therefore the angles used are unevenly spaced with regions of greatest variability in the phase function having more points. Table 5 gives a list of the zenith angles, the cosines of the zenith angles and the azimuthal angles in the solution grid.

The depth grid is likewise determined by the solution technique and so the number of depth points depends upon the optical depth of the atmosphere and the accuracy of solution required. For the cases involved in this work the number of depth points was 49 for clear cases and 77 for clouds. Details on the selection of angular and depth grids may be found in Barkstrom (Ref. 13) and Suttles (Ref. 14).

Treatment of the azimuthal variation involves use of an expansion of the radiance field in an M-term Fourier cosine series in the azimuthal angle,

$$L_\lambda (\mu, \phi) = \sum_{m=0}^{M} L_\lambda^m (\mu) \cos m\phi \tag{5}$$

In this formulation the lower boundary condition may be written

$$L_\lambda^m (-\mu) = r_\lambda (\mu) L_\lambda^m (\mu) + \frac{2\pi}{\varepsilon_m} \int_0^1 \rho_\lambda^m (-\mu; \mu') L_\lambda^m (\mu') \mu' \, d\mu'$$

$$+ \mu_0 E_{0,\lambda} \rho_\lambda^m (-\mu; \mu_0) e^{-\tau_{TOT}/\mu_0} \tag{6}$$

where the first term represents the specular reflection at the surface, the second term represents the diffuse reflection of diffusely incident radiation and the third term represents the diffuse reflection of the directly incident solar beam. The factor $\rho_\lambda^m(-\mu;\ \mu')$ is the Fourier cosine coefficient of the spectral, bidirectional reflectance of the surface whose values are given by

$$\rho_\lambda^m(\mu;\ \mu') = \frac{\varepsilon_m}{2\pi} \int_0^{2\pi} \rho_\lambda(\mu,\ \phi;\ \mu',\ \phi') \cos m(\phi - \phi')\, d(\phi - \phi') \tag{7}$$

where

$$\varepsilon_m = \begin{cases} 1, & \text{if } m = 0 \\ 2, & \text{if } m > 0 \end{cases} \tag{8}$$

and $\rho_\lambda(\mu,\ \phi;\ \mu',\ \phi')$ are the diffuse spectral bidirectional reflectance data.

Evaluation of these coefficients was accomplished through the use of a fast Fourier transform routine available on the NASA LaRC NOS Mathematical Library (Ref. 15). The bidirectional reflectance data for the land surfaces described earlier (forest, grass and savannah from Kriebel and desert from Davis and Cox) were used to assemble a data base of spectral Fourier coefficients which could then be used in the FD program. The data base was built by computing 128 terms in the Fourier series for each of the elements in the 15 by 15 angular matrix defined by $\rho_\lambda^m(\mu;\ \mu')$. This was repeated for each wavelength in the original data sets. Since the desert data of Davis and Cox was developed from a broad-band measurement, only one wavelength index was required. The amount of data which resulted was rather large and therefore in order to facilitate access to the data by the FD program, the data base was stored on a random access file which allows for much more rapid retrieval than the standard sequential access storage.

The specular reflection term in equation (6) was assumed to be negligible, except for the ocean surface in which it is a major contributor. The specular reflection from the ocean surface was assumed to obey a Fresnel reflection law which is described in Siegel and Howell (Ref. 7).

Figures 2 through 5 show some examples of the normalized spectral radiance reflected up at the top of the atmosphere as calculated using the FD model. Radiances are normalized to the value of the spectral radiant exitance at the top of the atmosphere. The radiance field is assumed to be symmetrical with respect to the principal plane. The spectrally integrated radiances (labeled as λ = TOTAL in the figures) are calculated numerically using

$$L_{TOTAL} = \sum_{n=2}^{73} \frac{1}{2} (L_n + L_{n-1}) (\lambda_n - \lambda_{n-1}) \tag{9}$$

where L_n is the monochromatic solution of the transfer equation for wavelength λ_n.

B. The Delta-Eddington Model:

The delta-Eddington approximation is considered to be an efficient and reasonably accurate approach for radiative transfer calculations of the spectral flux. The method, as developed by Shettle and Weinman (Ref. 3) and by Joseph et al. (Ref. 16), is based on Eddington's approximation in which the azimuthal average radiance is written as a two term expansion in the cosine of the zenith angle,

$$L(\tau, \mu) \cong L_o(\tau) + \mu L_1(\tau). \tag{10}$$

The next step is to assume that the phase function for scattering may be approximated by using a Dirac delta function for the forward scatter peak and a two term expansion in the scattering angle α:

$$P(\cos\alpha) \cong 2\, f\, \delta(1 - \cos\alpha) + (1 - f)\,(1 + 3g' \cos\alpha) \qquad (11)$$

where f is the fraction scattered into the forward direction and g' is the mean value of the cosine of the scattering angle (or the asymmetry factor). Under these assumptions and approximations, the radiative transfer equation for an atmosphere consisting of homogeneous layers, can be reduced to a pair of coupled ordinary differential equations which can then be solved in closed form.

Software to perform these calculations had already been set up by Suttles and Tiwari (Ref. 17) with subroutines detailing the solar spectral irradiance and the Earth-atmosphere properties shared in common with the FD model. This gave further justification to its use in computing the spectral fluxes for radiance data base.

IV. DATA PRODUCTS

The primary goal of this research effort is to provide a data base of short-wave, spectral radiance models which are to be used in algorithms to correct for spectral effects caused by the ERBE Scanner Instrument. As discussed above, it was decided to use a detailed finite difference model to derive a set of spectral bidirectional angular models for the required Earth scene types and to combine these with a set of spectral flux models computed using a delta-Eddington model to simulate typical atmospheric variabilities. These data files were prepared and delivered to the ERBE Inversion Working Group in October, 1984.

A. Spectral Bidirectional Angular Models:

The spectral correction algorithms required that the radiance data base be stored using the angular bin structure shown in Table 6. FD grid points located near the centers of the solar zenith angle bins were considered to be representative for the entire bin. The same was true for the 5 relative azimuth angle bins, i. e., the value for the angle grid point at the center was considered to be representative of the values over the entire bin. To match the viewing zenith angle bins however, it was decided to combine the radiance values at adjacent zenith angle grid points and to compute an average radiance value for the bin. Weighted sums of the radiances across the FD angle ranges as indicated in Table 6 were computed with the resulting average value being stored as the values for the appropriate bins. The radiance values were all normalized to the values of the spectral flux as indicated in equation (2) to obtain the bidirectional angular models.

These resulting models were stored on data files identified by the scene type and solar and solar zenith angle. Bidirectional angular model values were stored as 4 x 5 arrays (4 viewing zenith bins by 5 azimuth bins) for each of the 73 wavelength values from 0.25 to 5.0 μm. An example is shown in Figure 6.

B. Spectral Flux Models:

The spectral flux models were assembled in order to provide variability in the radiance models due to atmospheric variations. With atmospheric data coming from the TOVS models as discussed earlier, the spectral flux data files comprised 73 spectral flux values for 4 solar zenith angles (only 2 solar zenith angles for polar winter cases) and for 12 months of atmospheric data. Figure 7 shows an example of one month of data stored a one of the 29 data files which makeup the spectral flux models.

V. CONCLUDING REMARKS

The models of spectral radiance described in this report have been created with a specific purpose in mind, namely to aid in the determination of the ERBE Scanner spectral correction factors. The data base created herein provides the capability to simulate radiance fields over the most common Earth scene types for a large number of atmospheric conditions. The atmospheric properties have been derived from recent measurements and the bidirectional reflectance properties employed are as realistic as are currently available. These models may also form the basis for a number of studies involving the angular effects of surface reflection and effects of atmospheric variability.

The next level of detail which would be desired in further studies would involve the inclusion of wind-roughened ocean surface effects and the inclusion of embedded clouds within the atmosphere. These are being planned for the near future.

REFERENCES

1. Tarnopolskiy, V. I.: "Optical Characteristics of the Earth's Surface and Atmosphere from the Point of View of Remote Sensing of Natural Resources", NASA TM-75548, 1978.

2. Wark, D. Q.; Yamamoto, G. and Lienesch, J. H.: "Infrared Flux and Surface Temperature Determinations from Tiros Radiometer Measurements," NOAA Meteorological Satellite Laboratory, Report No. 10, 1962.

3. Shettle, E. P. and Weinman, J. A.: "The Transfer of Solar Irradiance Through Inhomogeneous Turbid Atmospheres Evaluated by Eddington's Approximation," J. Atmos. Sci., Vol. 27, No. 10, 1970, pp. 1048-1055.

4. Kriebel, K. T.: "Measured Spectral Bidirectional Reflection Properties of Four Vegetated Surfaces," Appl. Opt., Vol. 17, No. 2, 1978, pp. 253-259.

5. Davis, J. M. and Cox, S. K.: "Regional Properties of Angular Reflectance Models," Atmospheric Science Paper No. 338, Colorado State Univ., 1981.

6. Wiscombe, W. J. and Warren, S. G.: "Model for the Spectral Albedo of Snow," J. Atmos. Sci Vol. 37, No. 12, 1980, pp. 2712-2733.

7. Siegel, Robert and Howell, John R.: "Thermal Radiation Heat Transfer," NASA SP-164, Vol. I, 1968.

8. Morel, A.: "In-Water and Remote Measurements of Ocean Color," Boundary-Layer Meteorol., Vol. 18, 1980, p. 177.

9. McClatchey, R. A.; Fenn, R. W.;Selby, J. E. A. and Garing, J. S.: "Optical Properties of the Atmosphere," Environmental Research Papers, No. 331, Air Force cambridge Research Laboratories, AFCRL-70-0527, 1970.

10. Deepak, A. and Gerber, H. E., eds.: "Report of the Experts Meeting on Aerosols and Their Climatic Effects," World Climate Research Program, WCP-55 1983.

11. Kidwell, Katherine B., ed.: NOAA Polar Orbiter Data Users Guide, 1981.

12. Stephens, G. L: "Radiation Profiles in Extended Water Clouds," I: Theory. J. Atmos. Sci. Vol. 35, No. 11, 1978, pp 2111-2122.

13. Barkstrom, B. R.: "A Finite Difference Method of Solving Anisotropic Scattering Problems," J. Quant. Spec. and Rad. Trans., Vol. 16, No. 9, 1976, pp. 725-739.

14. Suttles, J. T.: "Anisotropy of Solar Radiation Leaving the Earth-Atmosphere Systems," Ph.D. Thesis, Old Dominion Univ. 1981.

15. Mathematical and Statistical Software at Langley, Central Scientific Computing Complex, Document N-3, April, 1984.

16. Joseph, J. H.; Wiscombe, W. J. and Weinman, J. A.: "The Delta-Eddington Approximation for Radiative Flux Transfer," J. Atmos. Sci., Vol. 33, No. 12, 1976, pp. 2452-2459.

17. Suttles, J. T. and Tiwari, S. N.: "Transfer of Solar Radiation in the Atmospheric," AIAA Paper 79-1038, June 1979.

TABLE 1. SURFACE TYPES AND REFLECTION DATA SOURCES

SURFACE	SPECTRAL ALBEDO DATA	ANGULAR BIDIRECTIONAL MODEL
Forest	Tarnopolskiy (Ref. 1) (forest winter species)	Kriebel (Ref. 4) (coniferous forest)
Grass	Tarnopolskiy (dry valley meadows)	Kriebel (pasture land)
Savannah	Kriebel	Kribel
Desert	Tarnopolskiy (sand, desert outcrop, rocks)	Davis & Cox (Ref. 5) (Saudi Arabian Empty Quarter)
Ice/Snow	Wiscombe & Warren (Ref. 6) (dry, old snow)	--- (assumed Lambertian)
Ocean	Morel (Ref. 8) (blue, desert water)	Siegel & Howell (Ref. 7) (Fresnel Law)

TABLE 2. TOVS METEOROLOGICAL DATA SITES AND ASSUMED SCENE TYPES FOR SIMULATION

SET NO.	SITE DESCRIPTION	LAT - LON	SCENE TYPE(s)
TOV1	Tropical Ocean - Pacific	20° N - 130° W	Ocean
TOV2	Tropical Ocean - Indian	$0°_{LAT}$ - 90° E	Ocean
TOV3	Tropical Land - Amazon Jungle	5° S - 60° W	Forest, Grass
TOV4	Tropical Desert - Sahara	22.5°N - 25° E	Desert, Savannah
TOV5	Tropical Desert - Saudi Arabia	20° N - 50° E	Desert
TOV6	Midlat Ocean - N. Atlantic	45° N - 40° W	Ocean
TOV7	Midlat Land - Midwest U. S.	40° N - 95° W	Grass, Savannah
TOV8	Midlat Snow - W. Canada	50° N - 110° W	Snow (Winter, Spring) Forest (Summer, Fall) Grass (Summer, Fall)
TOV9	Polar Ocean - North Sea	70° N - $0°_{LON}$	Ocean
TOV10	Polar Land - Siberia	67° N - 100° E	Snow (Winter, Spring) Forest (Summer, Fall)
TOV11	Polar Ice/Snow - Greenland	75° N - 40° W	Ice/Snow

TABLE 3. RADIANCE CASE LIST

SCENE	ATMOSPHERE	SOLAR ZENITH ANGLES (DEGREES)
Ocean	Tropical -- Mari, V = 5	33.4, 55.6, 69.7, 84.0
	Midlat Summer " V = 5	" " " "
	Midlat Winter " V = 23	" " " "
	Polar Summer " V = 23	" " " "
	Polar Winter " V = 23	- - 69.7, 84.0
Grass	Tropical -- Cont, V = 5	33.4, 55.6, 69.7, 84.0
	Midlat Summer " V = 5	" " " "
	Midlat Winter " V = 23	" " " "
Forest	Tropical -- Cont, V = 5	33.4, 55.6, 69.7, 84.0
	Midlat Summer " V = 5	" " " "
	Midlat Winter " V = 23	" " " "
	Polar Summer " V = 23	" " " "
	Polar Winter " V = 23	- - 69.7, 84.0
Savannah	Tropical -- Cont, V = 5	33.4, 55.6, 69.7, 84.0
	Midlat Summer " V = 5	" " " "
	Midlat Winter " V = 23	" " " "
Desert	Tropical -- Cont, V = 23	33.4, 55.6, 69.7, 84.0
Ice/Snow	Midlat Summer Cont, V = 5	33.4, 55.6, 69.7, 84.0
	Midlat Winter " V = 23	" " " "
	Polar Summer " V = 23	" " " "
	Polar Winter " V = 23	- - " "
Cloud/Ocean	Low Cloud, τ = 6	33.4, 55.6, 69.7, 84.0
	Middle Cloud, τ = 12	" " " "
	High Cloud, τ = 20	" " " "
Cloud/Land	Low Cloud, τ = 6	33.4, 55.6, 69.7, 84.0
	Middle Cloud, τ = 12	" " " "
	High Cloud, τ = 20	" " " "

TABLE 4. SPECTRAL FLUX CASE LIST

SCENE	LAT. ZONE	MONTHS	TOVS DATA[c]	SOLAR ZENITH ANGLES (DEGREES)
Ocean[a]	Tropical	Jul - Jun	TOV1	29.0, 51.3, 68.4, 82.8
	Tropical	Jul - Jun	TOV2	29.0, 51.3, 68.4, 82.8
	Midlat	Jul - Jun	TOV6	" " " "
	Polar	Jul - Jun	TOV9	- - 68.4°, 82.8°
Grass[a]	Tropical	Jul - Jun	TOV3	29.0, 51.3, 68.4, 82.8
	Midlat	Jul - Jun	TOV7	" " " "
	Midlat	Apr - Sep	TOV8	" " " "
Forest[a]	Tropical	Jul - Jun	TOV3	29.0, 51.3, 68.4, 82.8
	Midlat	Apr - Sep	TOV8	" " " "
	Polar	Apr - Sep	TOV10	" " " "
Savannah[a]	Tropical	Jul - Jun	TOV4	29.0, 51.3, 68.4, 82.8
	Midlat	Apr - Sep	TOV7	" " " "
Desert[b]	Tropical	Jul - Jun	TOV4	29.0, 51.3, 68.4, 82.8
	Tropical	Jul - Jun	TOV5	" " " "
Ice/Snow[b]	Midlat	Oct - Mar	TOV8	29.0, 51.3, 68.4, 82.8
	Polar	Oct - Mar	TOV10	- - 68.4, 82.8
	Polar	Apr - Sep	TOV11	29.0, 51.3, 68.4, 82.8
	Polar	Oct - Mar	TOV11	- - 68.4, 82.8

[a]Both clear and cloudy cases

[b]Clear cases only

[c]See Table 2

TABLE 5. ANGULAR SOLUTION GRID FOR FD MODEL

ZENITH ANGLES, θ (DEGREES)	COS (θ)
88.790	0.0211
84.039	0.1039
76.997	0.2250
69.748	0.3461
64.603	0.4289
61.741	0.4735
55.571	0.5654
45.573	0.7000
33.424	0.8346
22.098	0.9265
17.471	0.9539
14.592	0.9677
10.226	0.9841
5.541	0.9953
1.793	0.9995

AZIMUTHAL ANGLES, ϕ (DEGREES)
0.0
7.5
30.0
37.5
60.0
90.0
120.0
142.5
150.0
172.5
180.0

TABLE 6. ANGULAR BINS FOR SPECTRAL BIDIRECTIONAL MODELS

Solar Zenith Angle Bins

μ_o		θ_o (degrees)				
From	To	From	To	Diff.	Center	Nearest FD Point
1.00	0.75	0	41.4	41.4	29.0	33.4
0.75	0.50	41.4	60.0	18.6	51.3	55.6
0.50	0.25	60.0	75.5	15.5	68.4	69.7
0.25	0.00	75.5	90.0	14.5	82.8	84.0

Viewing Zenith Angle Bins

θ (degrees)					
From	To	Diff.	Center	FD Angle Range	Indices
0	30	30	15.0	1.8 - 22.4	15 - 10
30	45	15	37.5	33.4	9
45	60	15	52.5	45.6 - 55.6	8 - 7
60	90	30	75.0	61.7 - 88.8	6 - 1

Relative Azimuth Angle Bins

ϕ (degrees)			
From	To	Diff.	Center
0	15	15	7.5
15	60	45	37.5
60	120	60	90.0
120	165	45	142.5
165	180	15	172.5

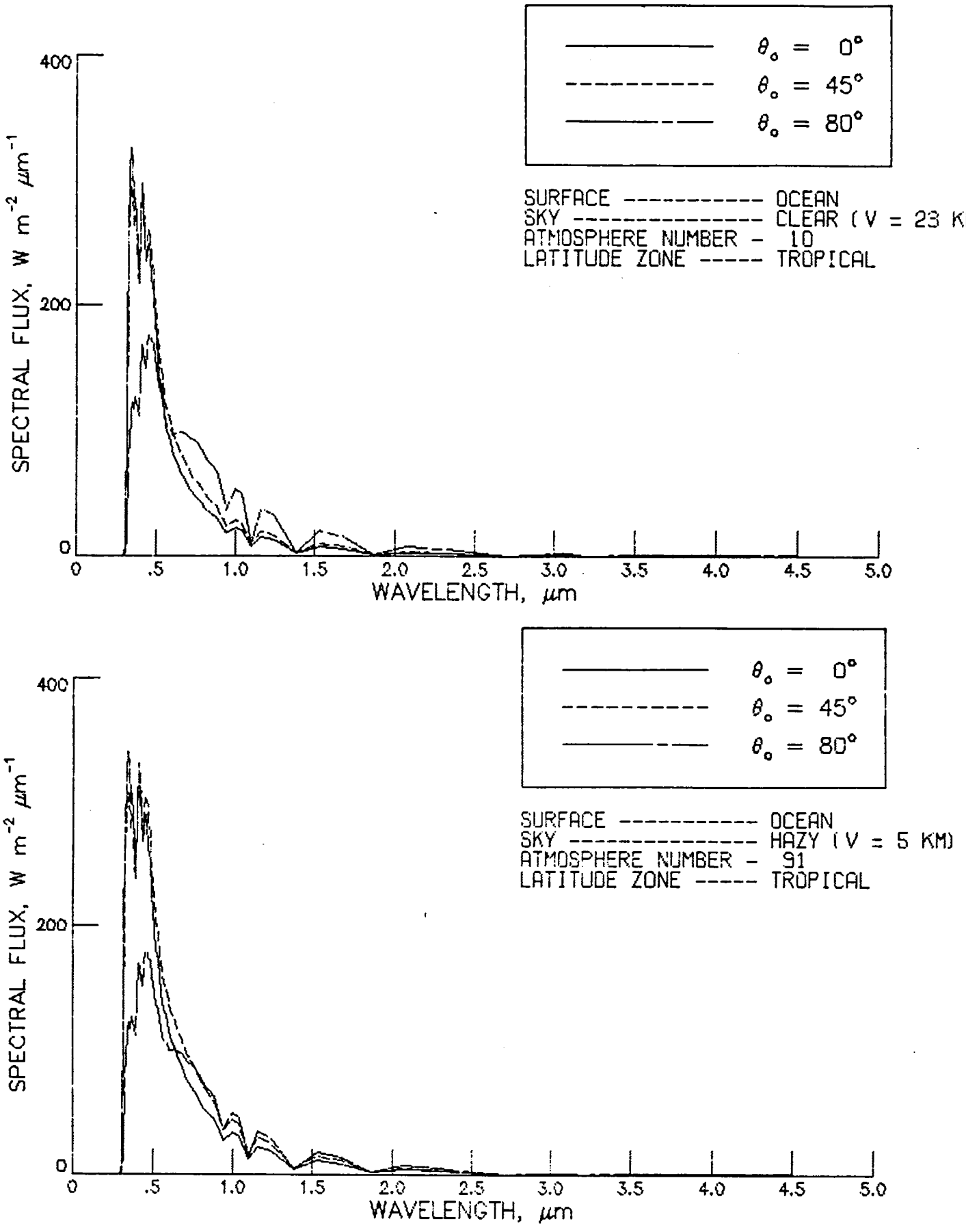

Figure 1. Sample of Top of Atmosphere Flux Spectra Used in Similarity Study.

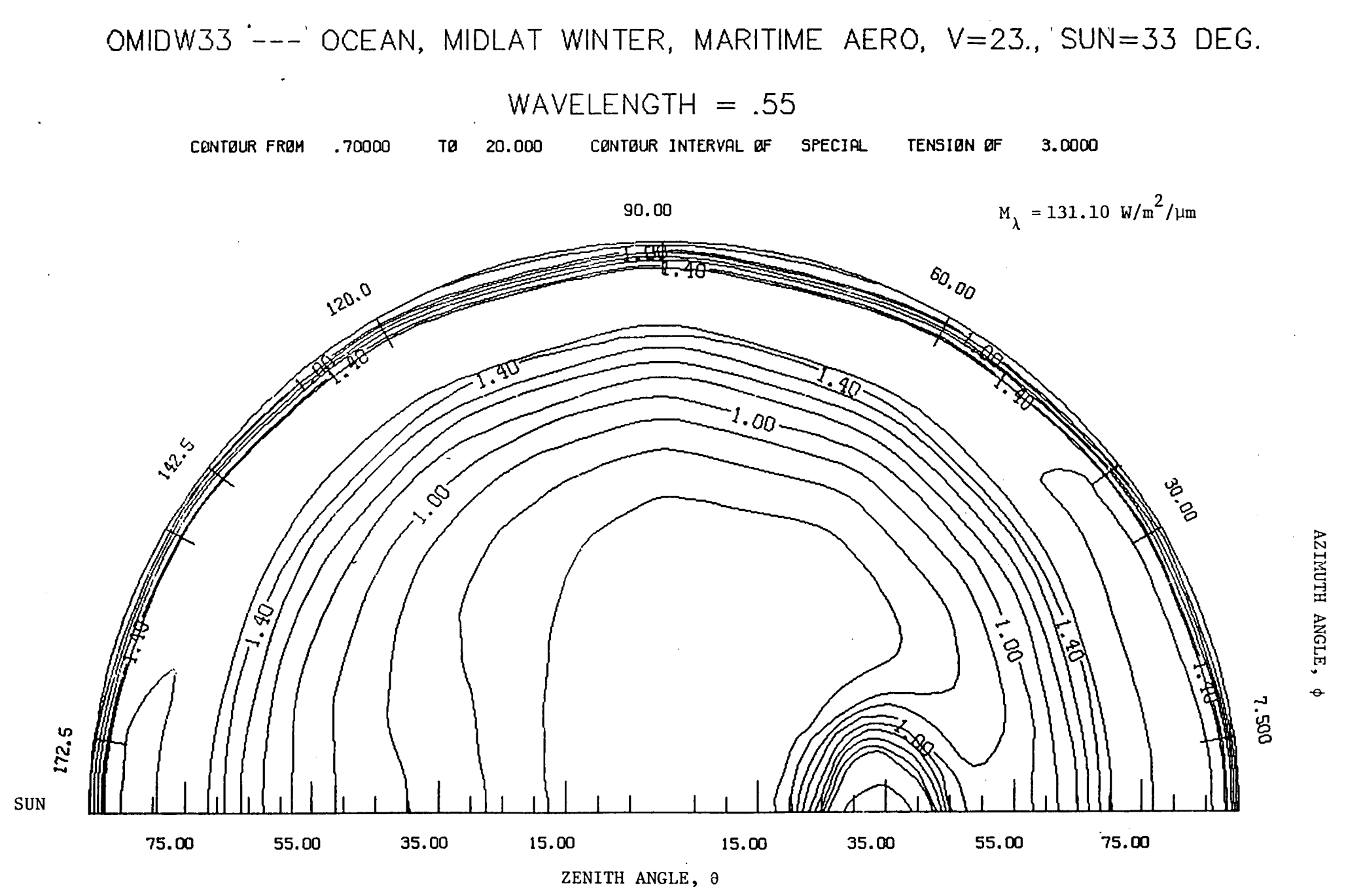

Figure 2. Normalized Top of Atmosphere Radiances for Ocean Surface, Midlatitude Winter, θ_o = 33.4° .

(a) λ = 0.55 μm

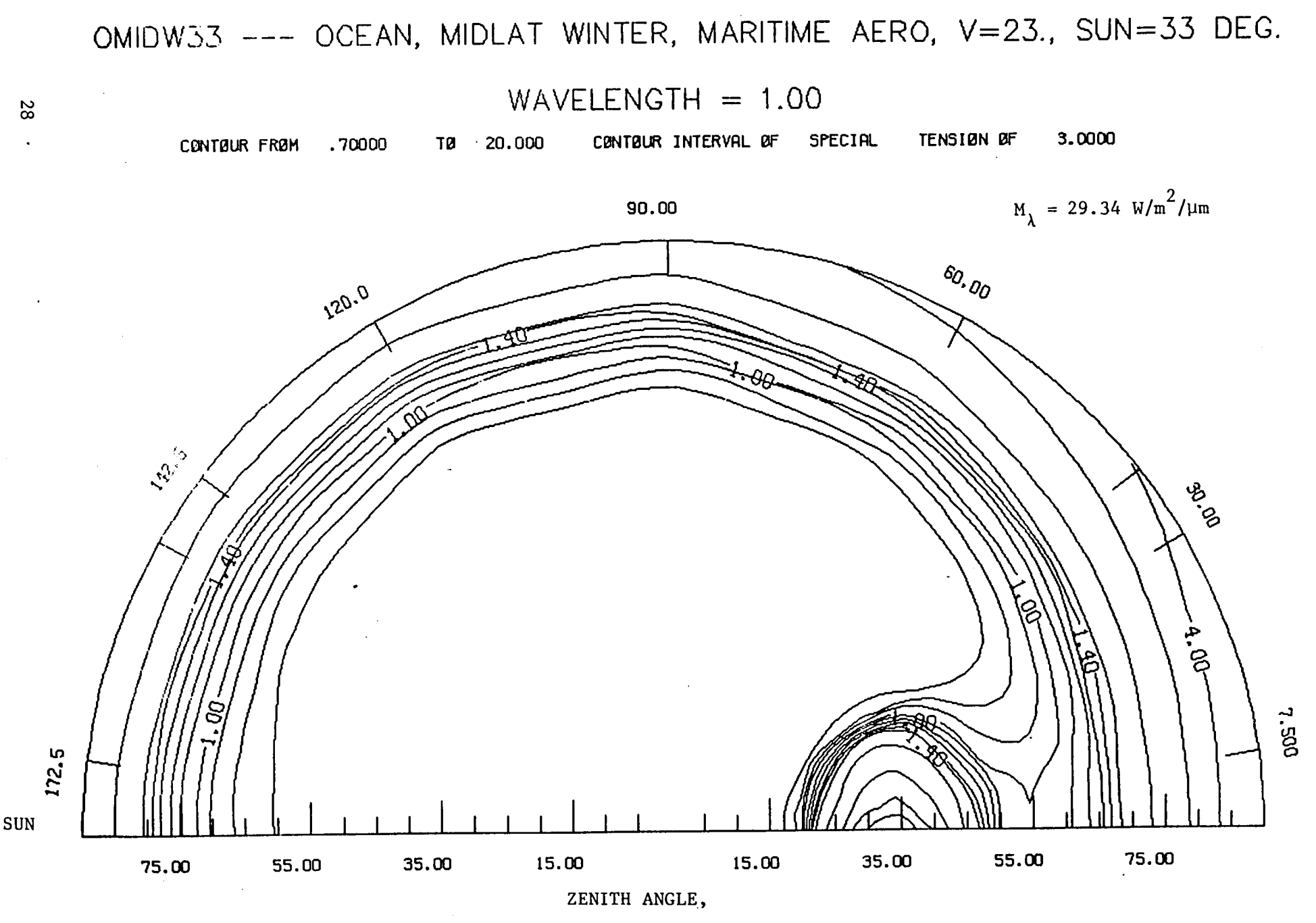

Figure 2. Normalized Top of Atmosphere Radiances for Ocean Surface, Midlatitude Winter, θ_o = 33.4°.

(b) λ = 1.00 μm

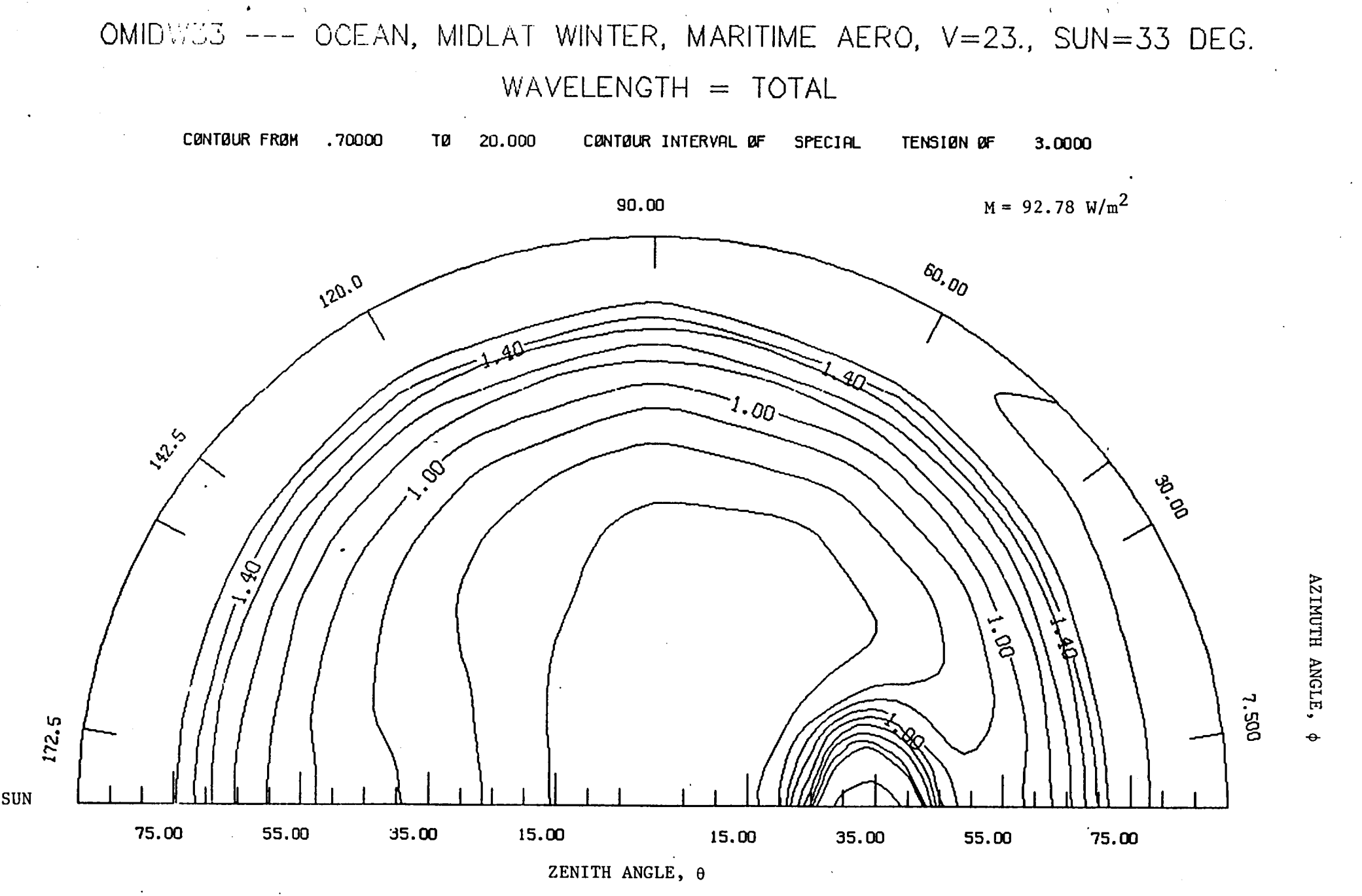

Figure 2. Normalized Top of Atmosphere Radiances for Ocean Surface, Midlatitude Winter, $\theta_o = 33.4°$.

(c) λ = TOTAL

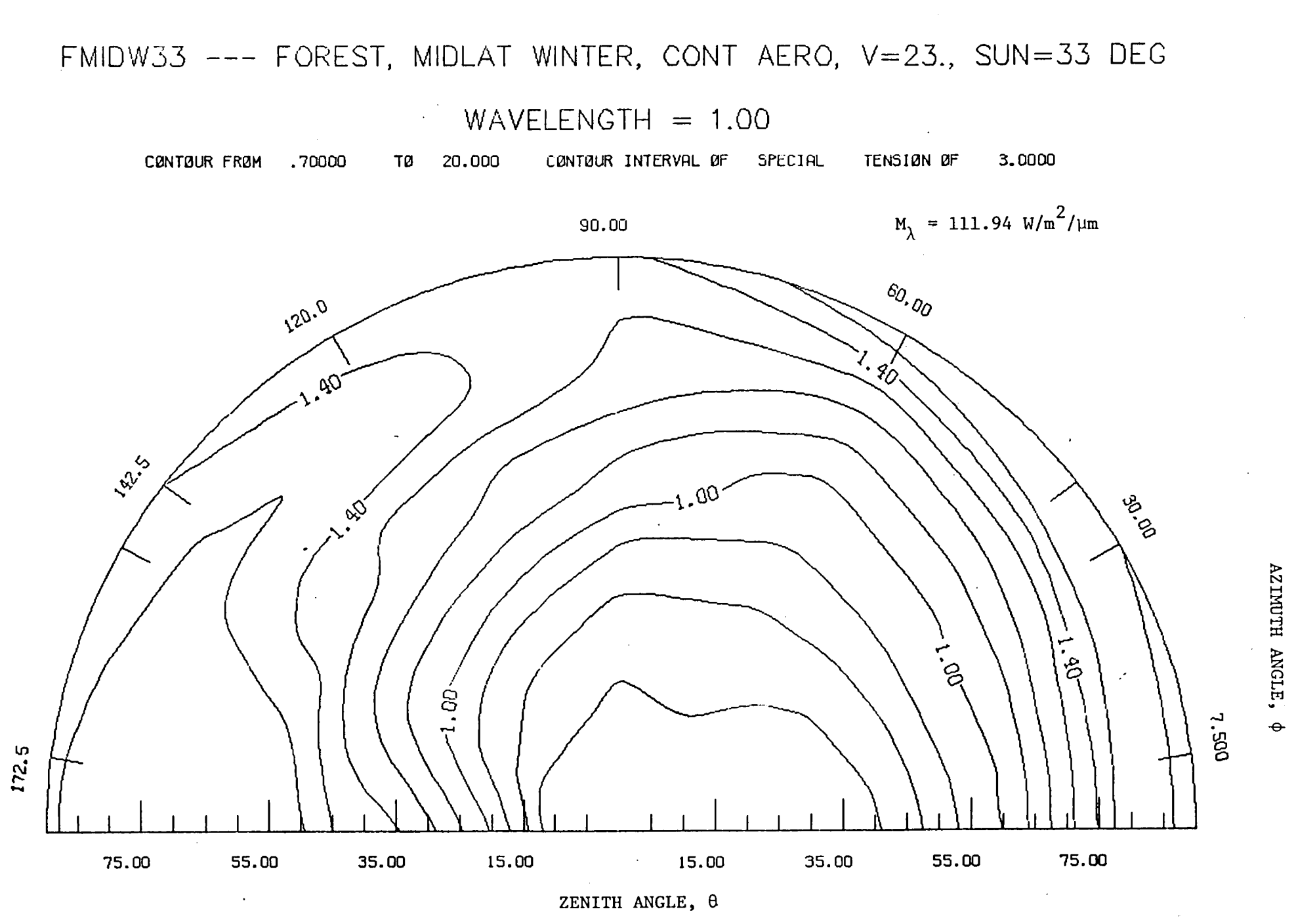

Figure 3. Same as Figure 2, Except for Forest Surface.

(a) λ = 0.55 μm

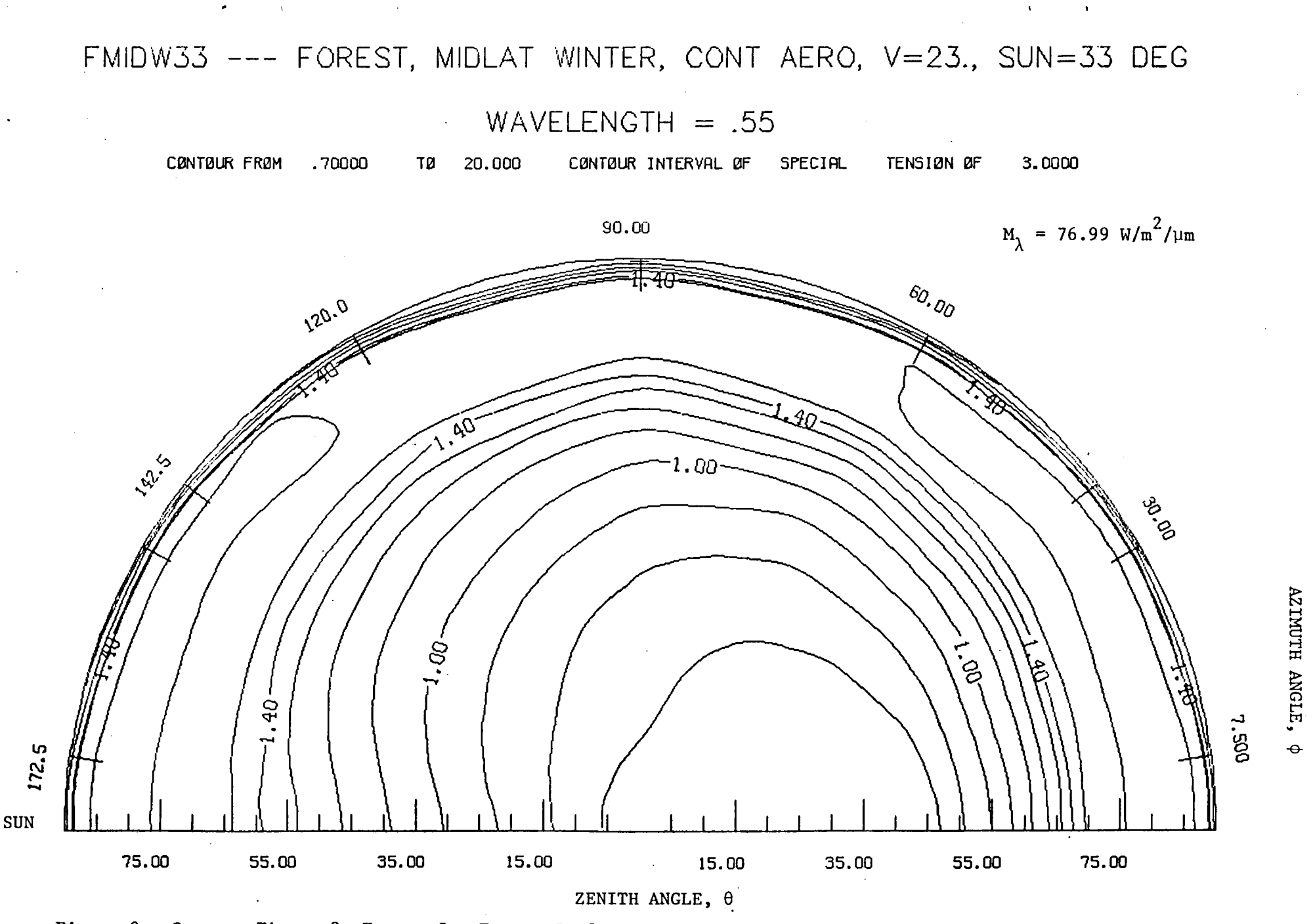

Figure 3. Same as Figure 2, Except for Forest Surface.

(b) λ = 1.00 μm

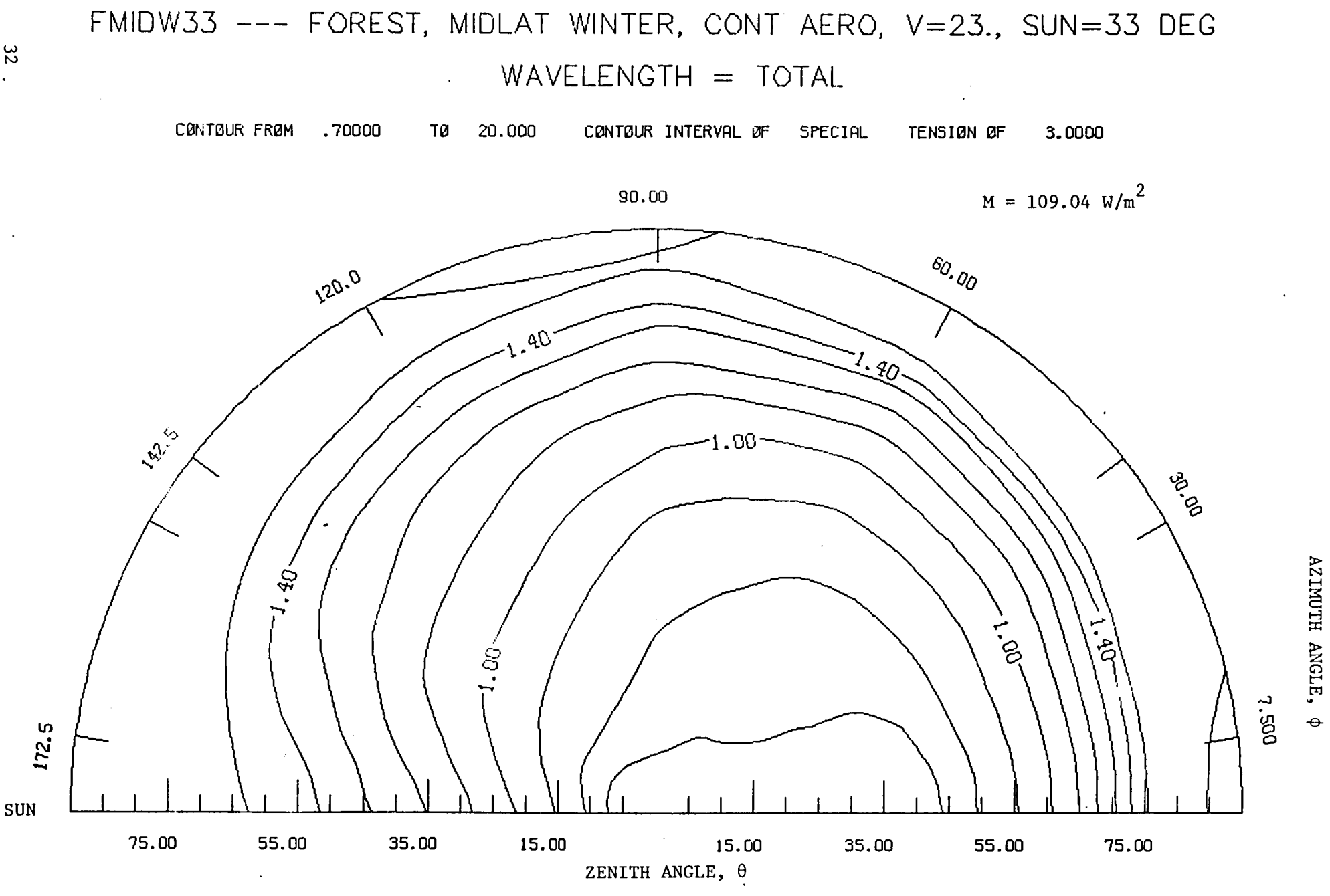

Figure 3. Same as Figure 2, Except for Forest Surface.

(c) λ = TOTAL

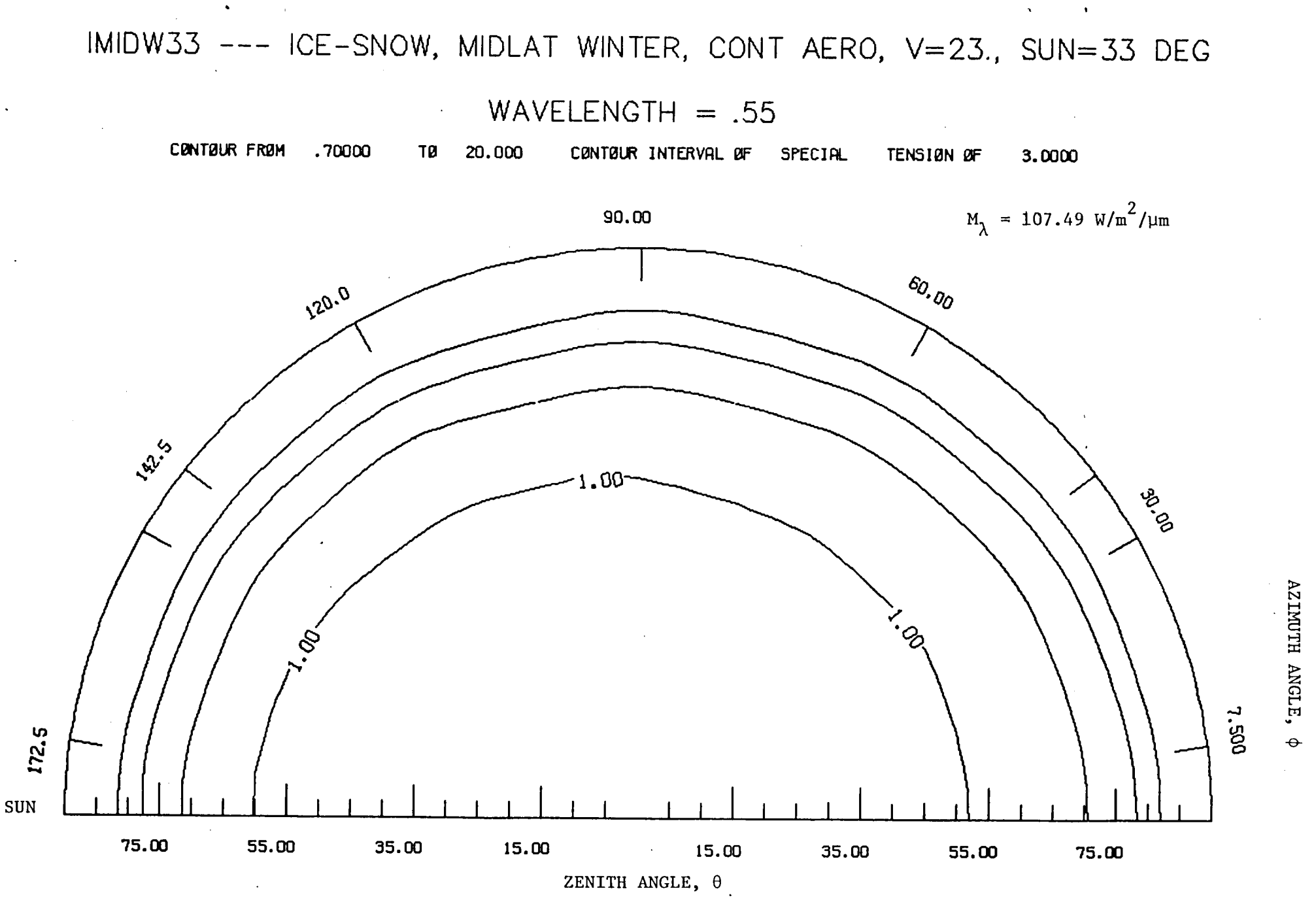

Figure 4. Same as Figure 2, Except for Ice/Snow Surface.

(a) λ = 0.55 μm

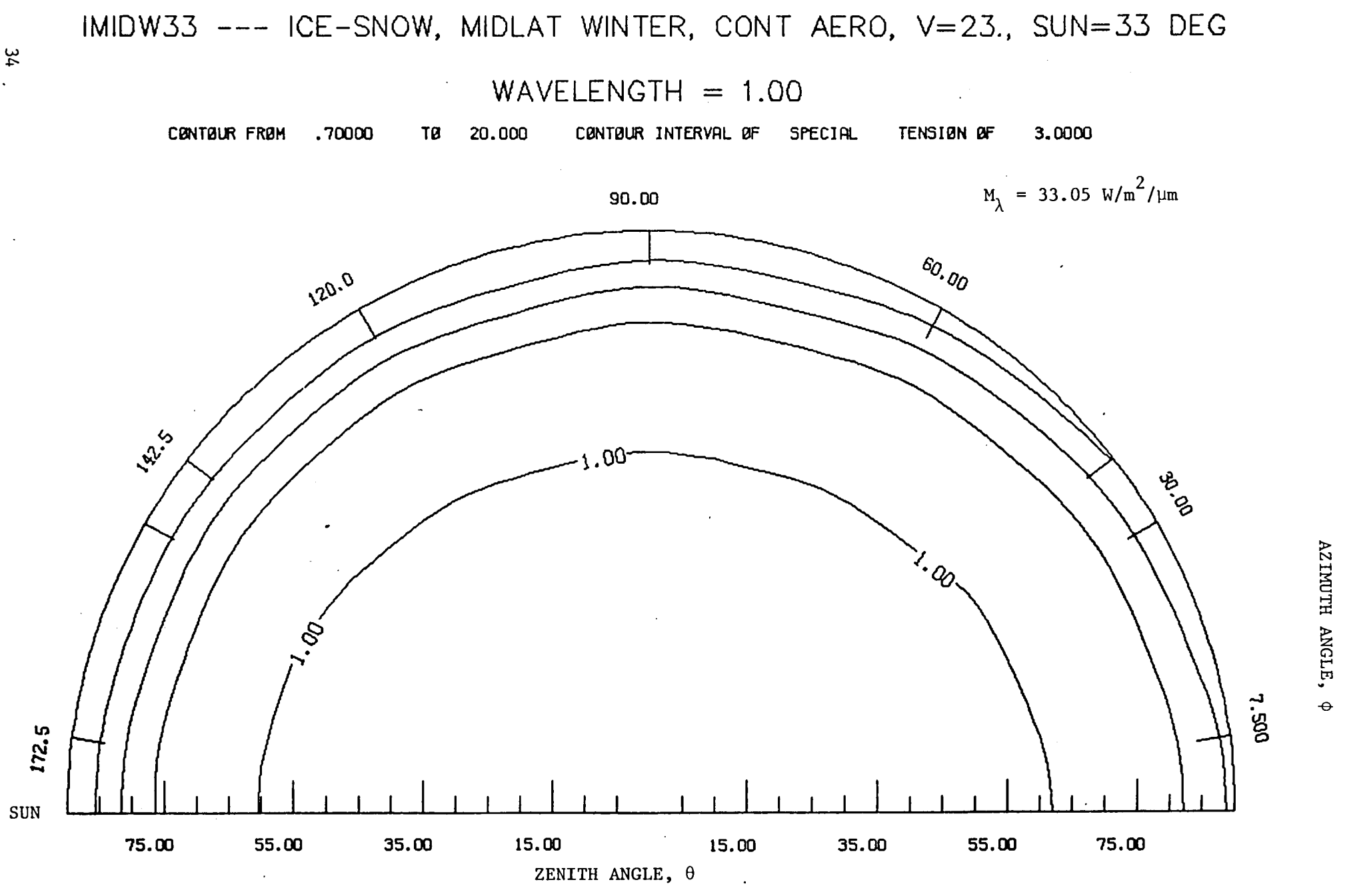

Figure 4. Same as Figure 2, Except for Ice/Snow Surface .

(b) λ = 1.00 μm

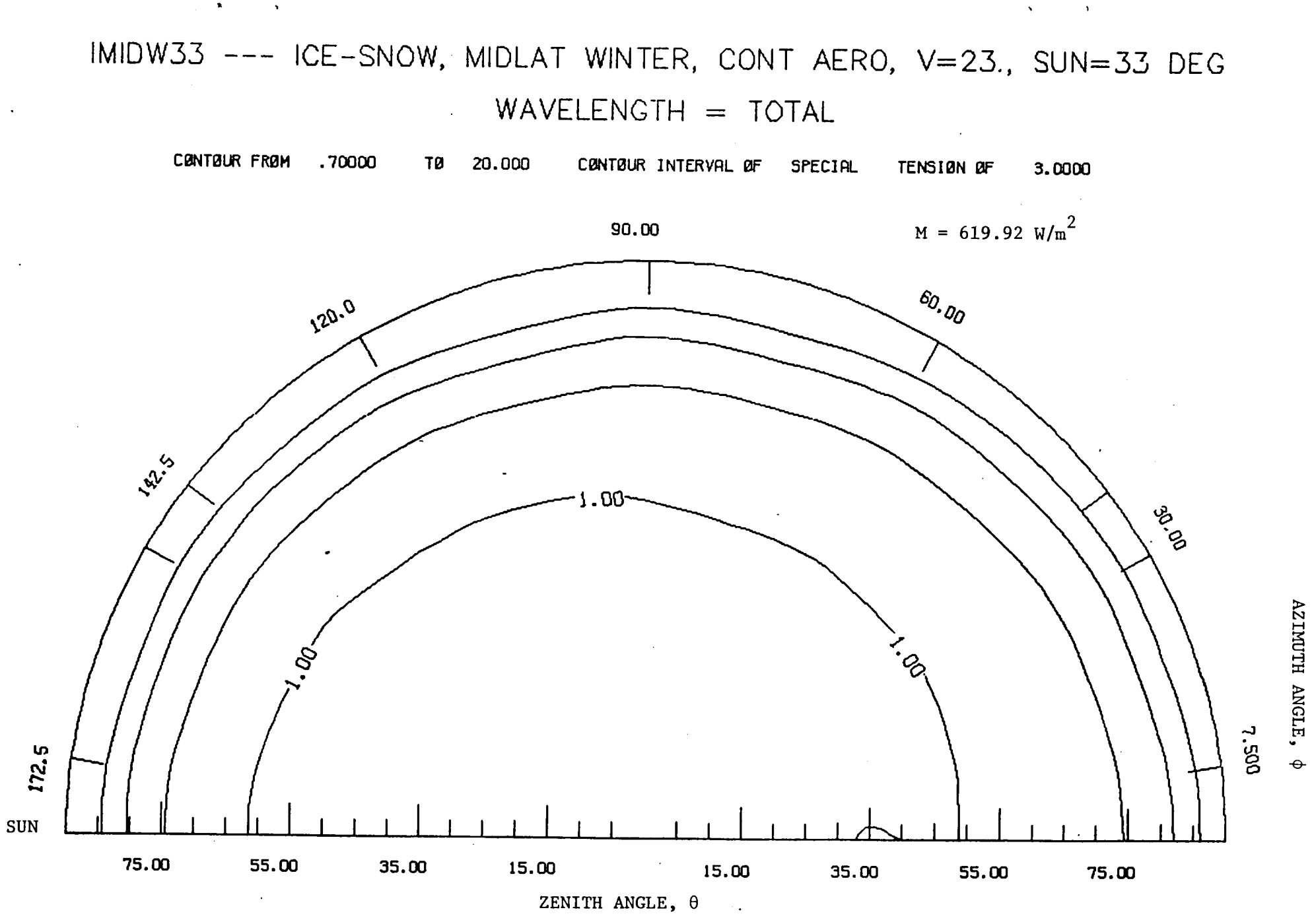

Figure 4. Same as Figure 2, Except for Ice/Snow Surface.

(c) λ = TOTAL

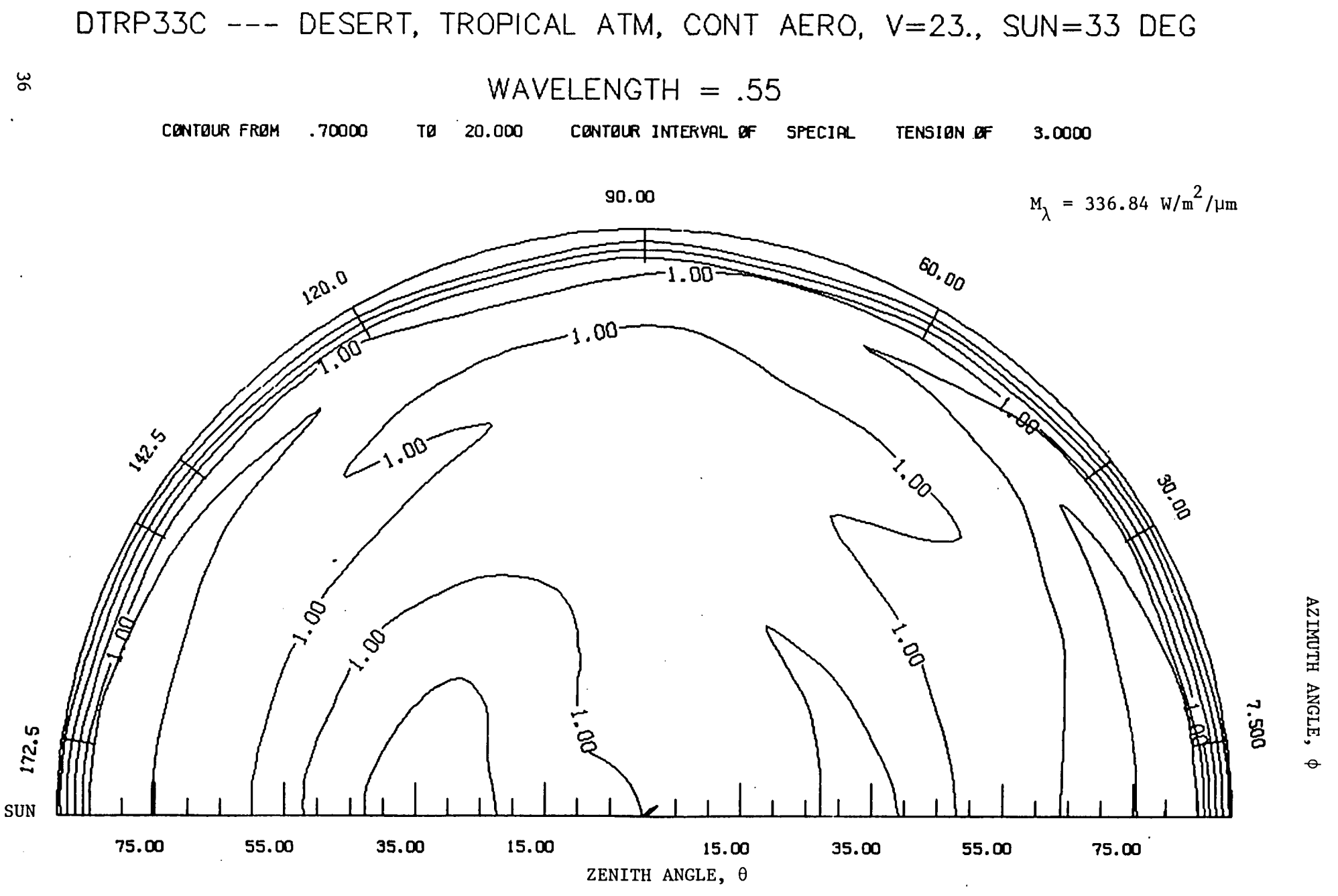

Figure 5. Same as Figure 2, Except for Desert Surface, Tropic.

(a) λ = 0.55 μm

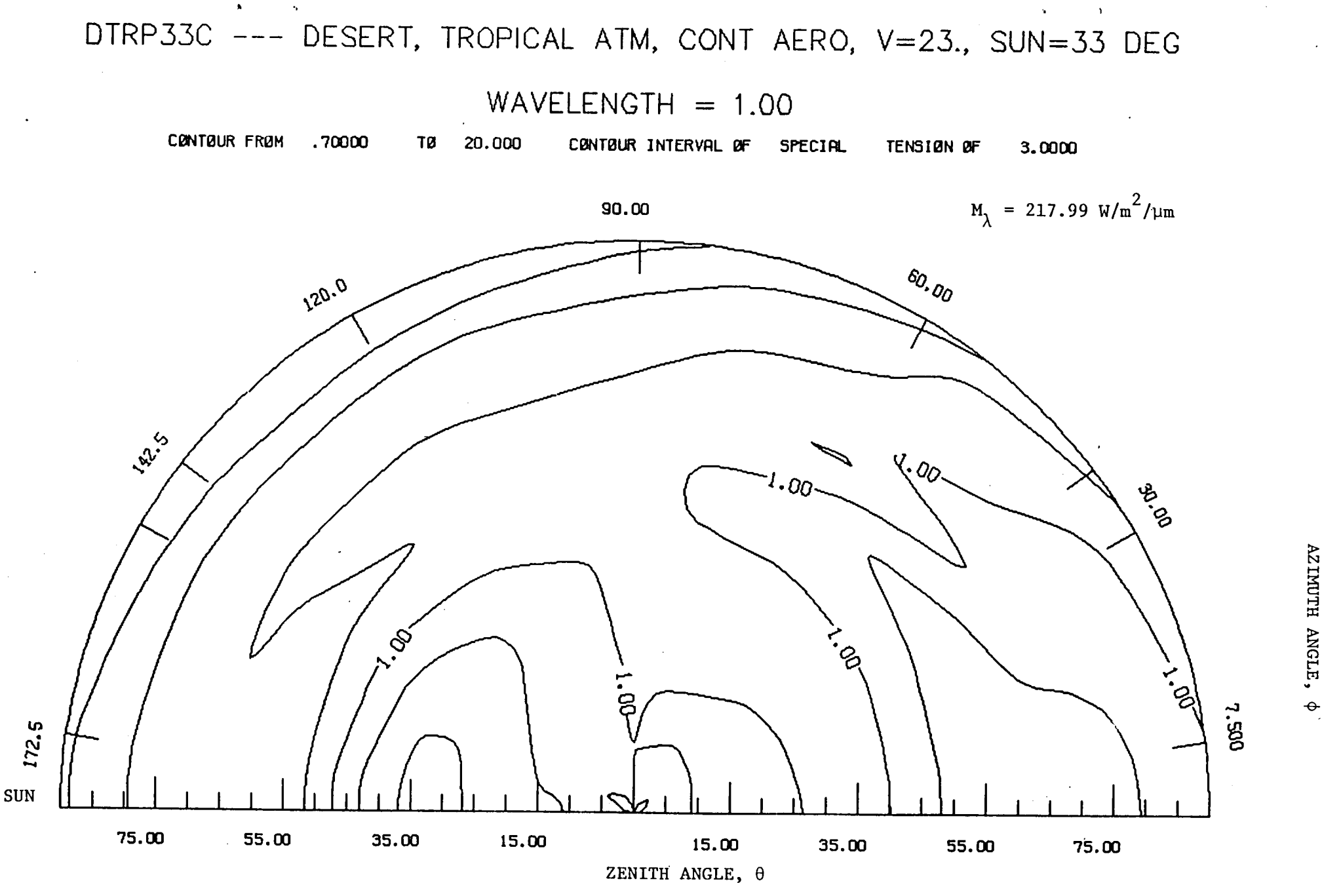

Figure 5. Same as Figure 2, Except for Desert Surface, Tropic.

(b) λ = 1.00 μm

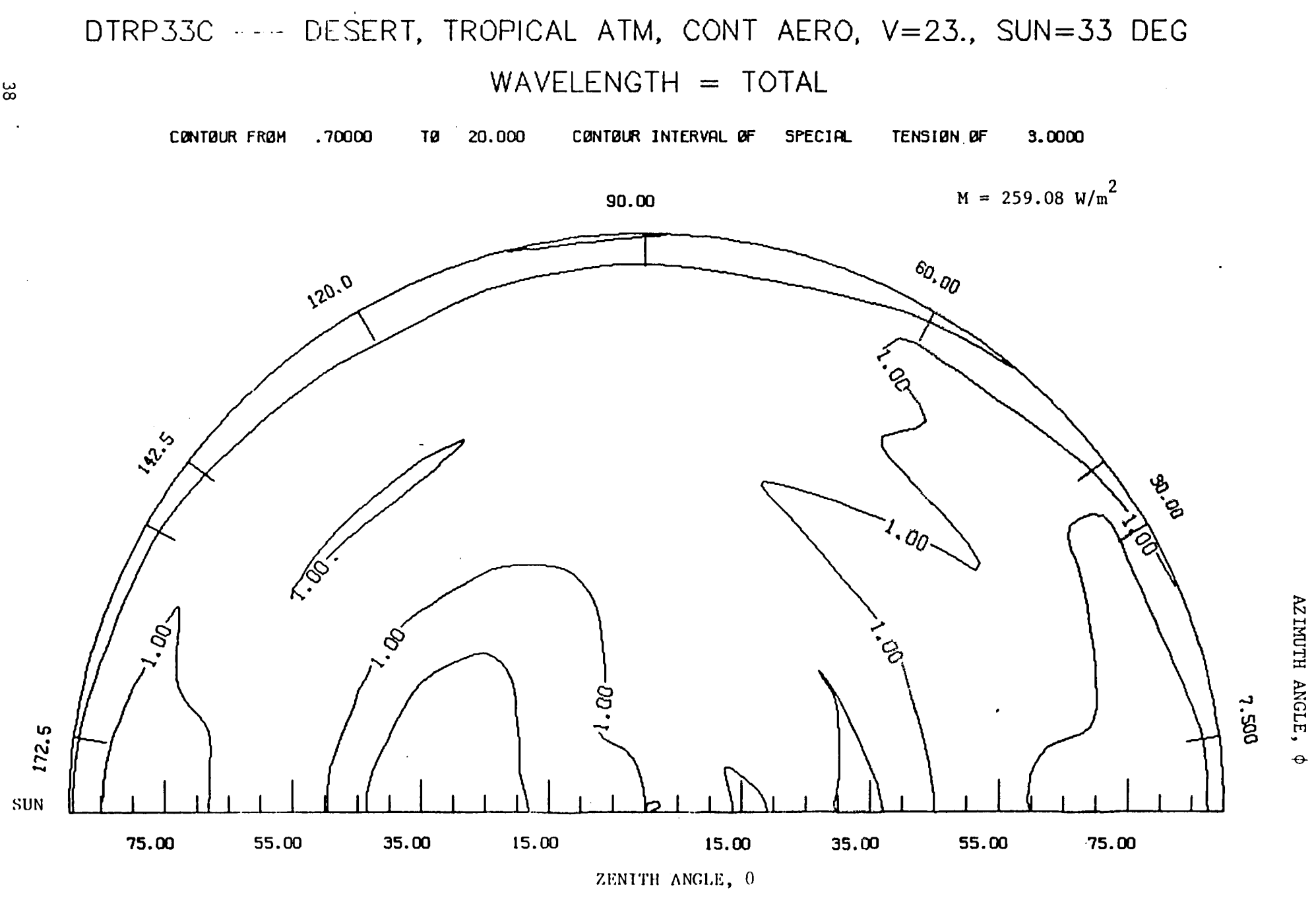

Figure 5. Same as Figure 2, Except for Desert Surface, Tropic.

(c) λ = TOTAL

SPECTRAL BIDIRECTIONAL MODEL, CASE:
FTROP33 --- FOREST, TROPICAL ATM, CONT AERO, V=5., SUN=33

WAVELENGTH = .250 MICRONS

ZENITH ---> / AZIMUTH	15.0	37.5	52.5	75.0
7.5	.686110E+00	.665506E+00	.797184E+00	.149019E+01
37.5	.700258E+00	.687770E+00	.792099E+00	.140367E+01
90.0	.763167E+00	.781843E+00	.861044E+00	.130011E+01
142.5	.842676E+00	.933609E+00	.107174E+01	.158257E+01
172.5	.865186E+00	.980580E+00	.114651E+01	.171328E+01

WAVELENGTH = .260 MICRONS

ZENITH ---> / AZIMUTH	15.0	37.5	52.5	75.0
7.5	.684320E+00	.659667E+00	.791936E+00	.149036E+01
37.5	.699029E+00	.684989E+00	.787819E+00	.140411E+01
90.0	.763099E+00	.781236E+00	.859657E+00	.130244E+01
142.5	.843674E+00	.934992E+00	.107302E+01	.158777E+01
172.5	.866451E+00	.982453E+00	.114844E+01	.171936E+01

WAVELENGTH = .270 MICRONS

ZENITH ---> / AZIMUTH	15.0	37.5	52.5	75.0
7.5	.682094E+00	.622105E+00	.726722E+00	.145346E+01
37.5	.700439E+00	.664009E+00	.735072E+00	.137561E+01
90.0	.777010E+00	.785093E+00	.844816E+00	.130871E+01
142.5	.870189E+00	.963337E+00	.109296E+01	.163243E+01
172.5	.896163E+00	.101693E+01	.117667E+01	.177420E+01

•
•
•

WAVELENGTH = 4.500 MICRONS

ZENITH ---> / AZIMUTH	15.0	37.5	52.5	75.0
7.5	.668334E+00	.720128E+00	.887937E+00	.125278E+01
37.5	.739086E+00	.806169E+00	.790538E+00	.105016E+01
90.0	.767395E+00	.810163E+00	.820117E+00	.940876E+00
142.5	.102191E+01	.127950E+01	.125204E+01	.110821E+01
172.5	.124898E+01	.190524E+01	.196388E+01	.146403E+01

WAVELENGTH = 5.000 MICRONS

ZENITH ---> / AZIMUTH	15.0	37.5	52.5	75.0
7.5	.667563E+00	.721474E+00	.887580E+00	.121850E+01
37.5	.740542E+00	.810116E+00	.787862E+00	.101971E+01
90.0	.768295E+00	.812877E+00	.820130E+00	.929309E+00
142.5	.102798E+01	.129201E+01	.126157E+01	.110538E+01
172.5	.126156E+01	.193640E+01	.199613E+01	.147445E+01

Figure 6. Sample of Spectral Bidirectional Angular Models.

JUL FOREST CONIFER SPECIES TROPIC V = 5. KM

SPECTRAL FLUX UP AT TOA, W M-2 MICRON-1

WAVELENGTH, MICRONS	SOLAR ZENITH ANGLE, DEGREES 29.0	51.3	68.4	82.8
.25000E+00	.13936E-01	.12068E-01	.90663E-02	.41610E-02
.26000E+00	.22489E-01	.19483E-01	.14644E-01	.67232E-02
.27000E+00	.47910E-01	.41618E-01	.31397E-01	.14452E-01
.28000E+00	.74361E-01	.64936E-01	.49485E-01	.23157E-01
.29000E+00	.35174E+00	.30783E+00	.23593E+00	.11381E+00
.29500E+00	.71737E+00	.62731E+00	.48031E+00	.23220E+00
.30000E+00	.10394E+01	.88944E+00	.67182E+00	.32292E+00
.30500E+00	.48334E+01	.31855E+01	.17204E+01	.71289E+00
.31000E+00	.27970E+02	.18826E+02	.81870E+01	.16312E+01
.31500E+00	.81541E+02	.61747E+02	.32639E+02	.52107E+01
.32000E+00	.13615E+03	.11023E+03	.66868E+02	.13956E+02
.32500E+00	.20635E+03	.17482E+03	.11673E+03	.32703E+02
.33000E+00	.25174E+03	.21913E+03	.15462E+03	.52108E+02
.34000E+00	.27113E+03	.24337E+03	.18179E+03	.73291E+02
.35000E+00	.26607E+03	.24297E+03	.18628E+03	.79565E+02
.36000E+00	.24457E+03	.22632E+03	.17653E+03	.77150E+02
.37000E+00	.25390E+03	.23792E+03	.18851E+03	.83925E+02
.38000E+00	.22611E+03	.21445E+03	.17246E+03	.78081E+02
•				
•				
•				
.18700E+01	.26360E+01	.21465E+01	.13640E+01	.37203E+00
.20700E+01	.65643E+01	.59432E+01	.48215E+01	.27076E+01
.23000E+01	.51328E+01	.45730E+01	.36181E+01	.19200E+01
.27000E+01	.35959E-01	.27107E-01	.16220E-01	.70253E-02
.30000E+01	.14108E+01	.12618E+01	.10062E+01	.54984E+00
.31000E+01	.12035E+01	.10812E+01	.86913E+00	.48666E+00
.32000E+01	.32358E-01	.23845E-01	.13442E-01	.48394E-02
.35000E+01	.69290E+00	.62781E+00	.51218E+00	.29862E+00
.40000E+01	.43686E+00	.39274E+00	.31659E+00	.17995E+00
.45000E+01	.26612E+00	.23785E+00	.18985E+00	.10513E+00
.50000E+01	.17041E+00	.15153E+00	.11994E+00	.65040E-01
TOTAL FLUX	.12688E+03	.12437E+03	.10591E+03	.52683E+02
ALBEDO	.111818	.153326	.221757	.323994

Figure 7. Sample of Spectral Flux Models.

1. Report No.	2. Government Accession No.	3. Recipient's Catalog No.
NASA CR-172595		

4. Title and Subtitle	5. Report Date
SOLAR RADIANCE MODELS FOR DETERMINATION OF ERBE SCANNER FILTER FACTORS	May 1985
	6. Performing Organization Code
7. Author(s)	8. Performing Organization Report No.
Robert F. Arduini	685101
	10. Work Unit No.
9. Performing Organization Name and Address	11. Contract or Grant No.
Information and Control Systems, Inc. 28 Research Drive Hampton, Virginia 23666	NAS1-17425
	13. Type of Report and Period Covered
12. Sponsoring Agency Name and Address	Contractor Report
National Aeronautics and Space Administration Washington, DC 20546	14. Sponsoring Agency Code 619-12-30-01

15. Supplementary Notes

Langley Technical Monitor: John T. Suttles
Interim Report

16. Abstract

The purpose of this effort has been to provide shortwave spectral radiance models for use in the spectral correction algorithms for the ERBE Scanner Instrument. The required data base was delivered to the ERBE Data Reduction Group in October 1984. It consisted of two sets of data files: (1) the spectral bidirectional angular models and (2) the spectral flux models. The bidirectional models embody the angular characteristics of reflection by the Earth-atmosphere system and were derived from detailed radiance calculations using a finite difference model of the radiative transfer process. The spectral flux models were created through the use of a delta-Eddington model to economically simulate the effects of atmospheric variability. By combining these data sets, a wide range of radiances may be approximated for a number of scene types.

17. Key Words (Suggested by Author(s))	18. Distribution Statement
Earth Reflected Radiance Bidirectional Reflectance Spectral Radiance Shortwave Radiance	Unclassified - Unlimited Subject Category 47

19. Security Classif. (of this report)	20. Security Classif. (of this page)	21. No. of Pages	22. Price*
Unclassified	Unclassified	46	A03